

# CAD-based simulation of the hobbing process for the manufacturing of spur and helical gears

V. Dimitriou · A. Antoniadis

Received: 20 May 2007 / Accepted: 28 February 2008 / Published online: 29 April 2008  
© Springer-Verlag London Limited 2008

**Abstract** Targeting an accurate and realistic simulation of the gear hobbing process, we present an effective and factual approximation based on three-dimensional computer-aided design. Hobbing kinematics is directly applied in one gear gap. Each generating position formulates a spatial surface path which bounds its penetrating volume into the workpiece. The three-dimensional surface paths generated from the combination of the relative rotations and displacements of hob and work gear are used to split the subjected volume, creating concurrently the chip and the remaining work gear solid geometries. The developed software program HOB3D simulates accurately the manufacturing of spur and helical gears, exploiting the modeling and graphics capabilities of a commercial CAD software package. The resulting three-dimensional solid geometrical data, chips and gears provide the whole geometrical information needed for further research, such as prediction of the cutting forces, tool stresses and wear development as well as the optimization of the gear hobbing process.

**Keywords** Gear hobbing · Manufacturing simulation · CAD modeling

## 1 Introduction

Gear hobbing is a widely applied manufacturing process for the construction of any external tooth form developed

uniformly about a rotation center. Compared to conventional machining, such as turning and milling, the hobbing process is a sophisticated metal removal technology. While it is the most widely used process for the roughing of gears, its complexity and cost keep this technique poorly known. The kinematics principle of the process is based on three relative motions between the workpiece and the hob tool. For the production of spurs or helical gears, the workpiece rotates about its symmetry axis with a certain constant angular velocity, synchronized with the relative gear hob rotation. The worktable or the hob may travel along the work axis with the selected feed rate, depending on the hobbing machine that is used.

For the simulation of the gear hobbing process variant approximations have been proposed for the development of numerical and analytical models, aiming at the determination of the undeformed chip geometry, cutting force components and tool wear development [1, 2]. The industrial weight of these three simulation results is associated with the optimization of the efficiency per unit cost of the gear hobbing process. The undeformed chip geometry is an essential parameter to determine the cutting force components, as well as to predefine the tool wear development, both of them important cost related data of hobbing process [3]. For the effective specification of the tolerances on hob design parameters and allowable alignment errors, Kim [4] proposes a method of representing the geometry of a hob tooth profile in parametric form and of determining the surface equation of a generated gear as a function of hob design parameters and generating motion specifications through a mathematical model of the generation process. The simulation of meshing of face hobbled spiral bevel and hypoid gears and mathematic models of tooth surface generations are presented by Fan, and a tooth contact analysis program was developed [5].

---

V. Dimitriou  
Technological Educational Institute of Crete,  
Chania, Crete, Greece

A. Antoniadis (✉)  
Technical University of Crete,  
Chania, Crete, Greece  
e-mail: antoniadis@dpem.tuc.gr

The research work presented in [6–11] provided the basic knowledge for the numerical modeling of the gear hobbing process and later on newer approximations were proposed based on a similar modeling strategy [12–17]. These approximation methods are proposed for the determination of the hobbing process results, but the main characteristic of these methods is the reduction of the actual three-dimensional process to planar models, primarily for simplification reasons. The application of these former approximations is leading to planar results, without to represent the exact solid geometry of the real chips and gears, with accuracy directly dependent from various input parameters such as the number of the calculation planes. Furthermore, any post-processing of the extracted chip and gear planar geometries, e.g., finite element analysis, requires additional data processing which leads to supplementary interpolations of the two-dimensional results.

Focusing on the realistic and accurate simulation of the gear hobbing process, without inevitable modeling insufficiencies, we present an approach for the simulation of manufacturing spur and helical gears in this research work. A software program called HOB3D, originally presented in [18], is used for the guidance of an existent commercial CAD system, exploiting its powerful modeling and graphics capabilities. HOB3D is built in terms of a computer code in Visual Basic, extending this capability to other cutting processes based on the same cutting principle. The resulting solid models output formats offer realistic parts, chips and work gears, easily managed for further individual research or as an input to any other CAD, CAM or FEA commercial software systems.

## 2 HOB3D modeling procedure

The rolling principle between the hob and the workpiece makes the gear hobbing process different from conventional milling. As presented in Fig. 1, the process problem is basically prescribed from the geometrical characteristics of the gear to be cut, the hob that will be used and the involved kinematics between them.

The geometry of a resulting gear is basically described by six parameters: module ( $m$ ), number of teeth ( $z_2$ ), outside diameter ( $d_g$ ), helix angle ( $h_a$ ), gear width ( $W$ ) and pressure angle ( $a_n$ ). The correlation of these parameters automatically yields the module ( $m$ ) of the hob tool, whereas other tool geometrical parameters as external diameter ( $d_h$ ), number of columns ( $n_c$ ), number of origins ( $z_1$ ), axial pitch ( $\epsilon$ ) and helix angle ( $\gamma$ ), are options to be chosen.

As soon as the geometrical parameters of the two combined parts are set, the kinematics chain has to be initialized. The helix angle of the hob and the work gear prescribe the setting angle ( $\theta_s$ ) between the parts and the way that their relative motions will take place. Three

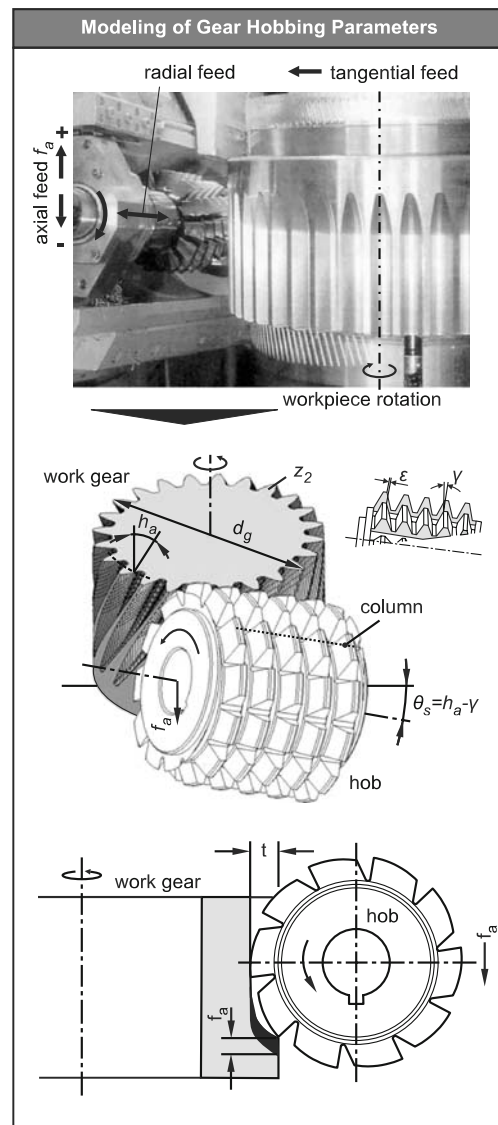
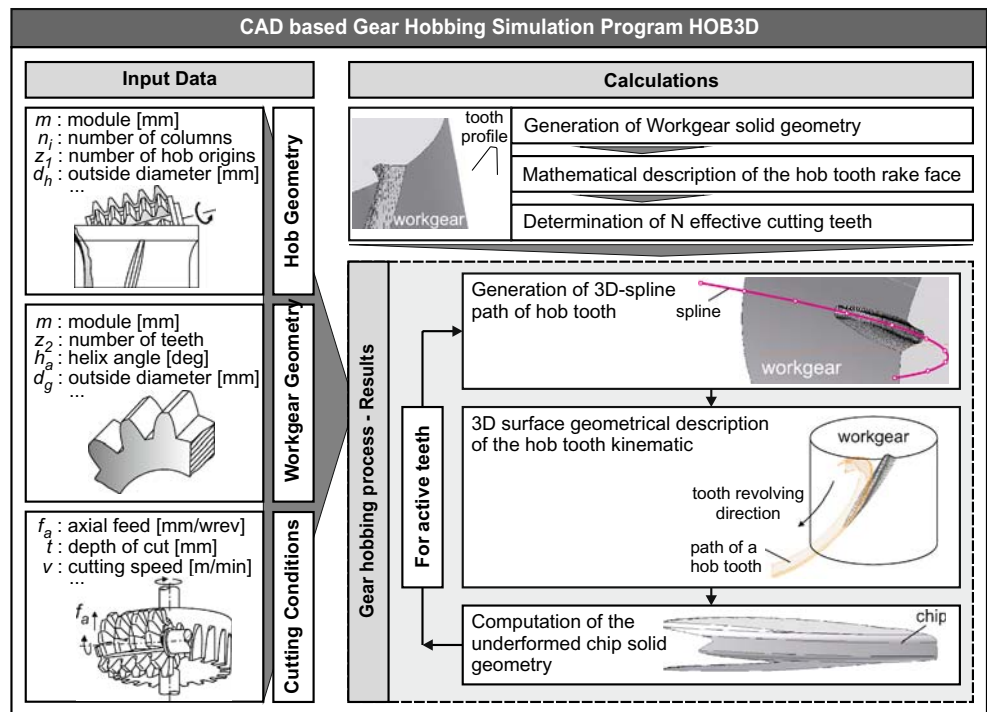


Fig. 1 Essential parameters of gear hobbing

distinct cutting motions are required: the tool rotation about its axis, the tool axial displacement and the workpiece revolution about its axis. By these means, the direction of the axial feed ( $f_a$ ) prescribes two different hobbing strategies: the climb (CL) and the up-cut (UC). In case of helical gears, two additional variations exist, the tool helix angle ( $\gamma$ ) compared to the helix of the gear ( $h_a$ ). If the direction of the gear helix angle is identical to the hob helix angle the type of the process is set to equi-directional (ED), if not to counter-directional (CD) one.

As presented in Fig. 2, after the initialization of the input data the solid geometry of the work gear is created in the CAD environment and one hob tooth rake face profile is mathematically and visually formed. At the same moment the assembly of the effective cutting hob teeth ( $N$ ) is determined and the kinematics of gear hobbing process is directly applied in one three-dimensional tooth gap of the

**Fig. 2** Flowchart of the program HOB3D



gear due to the axisymmetric configuration of the problem. Moreover, a three-dimensional surface is formed for every generating position (e.g., successive teeth penetrations), combining the allocation of the hob and the work gear, following a calculated spatial spline as a rail. These three-dimensional surface paths are used to identify the undeformed chip solid geometry, to split the subjected volume and to create finally the chip and the remaining work gear solid geometries.

### 3 HOB3D simulation strategy

In this approach every rotation and displacement that is taking place between the hob and the work gear during the simulation of the process are directly transferred to the hob. As presented in Fig. 3, the global coordinate system of the two parts is fixed to the center of the upper base of the workpiece, providing a steady reference system to the travelling hob. The presented scheme of kinematics has been adopted and in previous numerical approximation research works, mentioned at the introduction.

Without any loss of generality, the hob is considered to have a tooth numbered-named: Tooth 0. The identification vector  $v_0$  of Tooth 0 has its origin  $C_H$  on the  $Y_h$  axis of the hob and its end at the middle of the rake face, forming a module that equals to  $d_h/2$ . This vector determines the direction of the  $Z_h$  axis of the hob coordinate system  $X_h Y_h Z_h$  and is initially placed as an offset of the global Z-axis, set at a vertical distance  $L_1$  from the origin of the

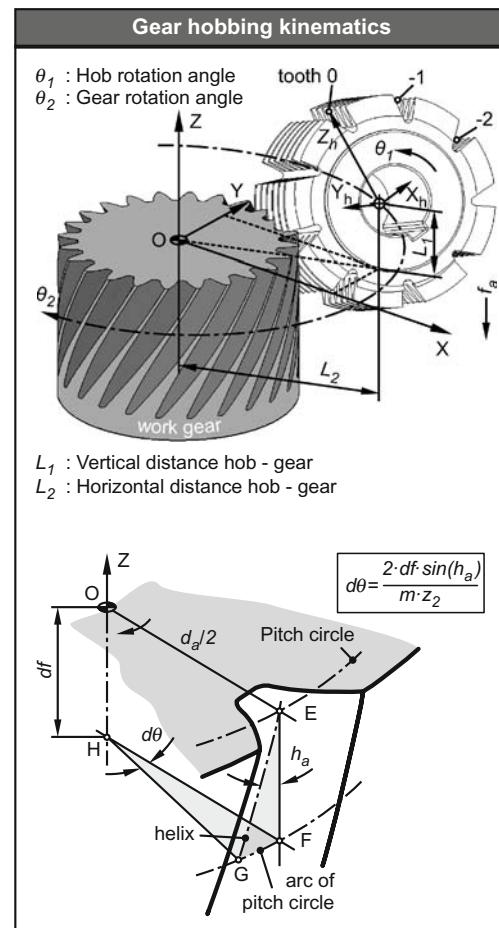


**Fig. 3** HOB3D simulation kinematics scheme

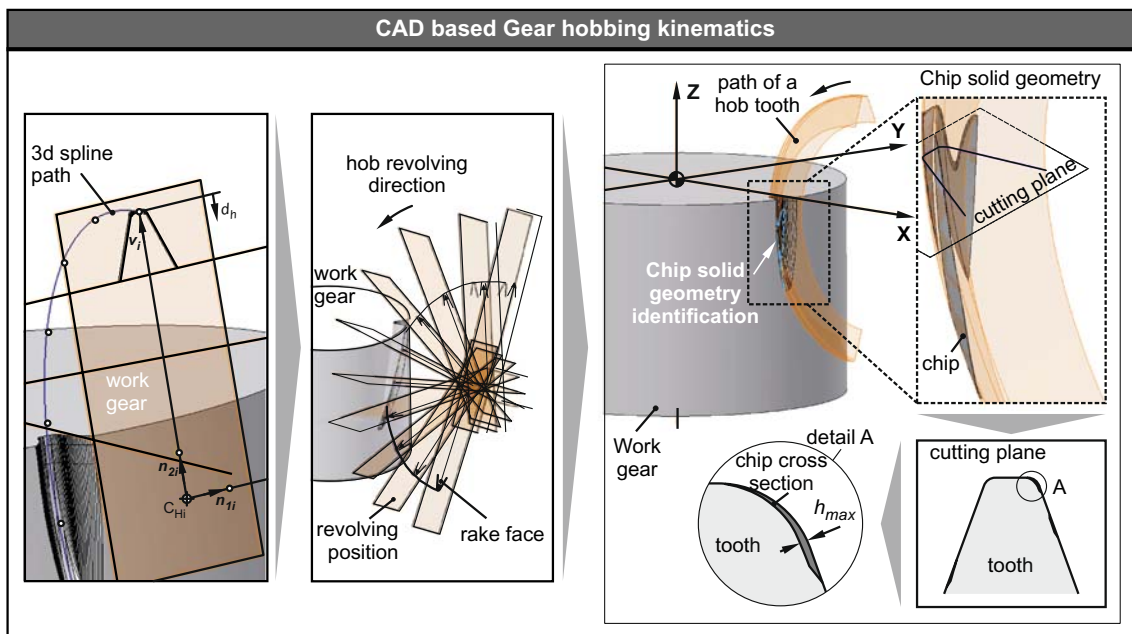


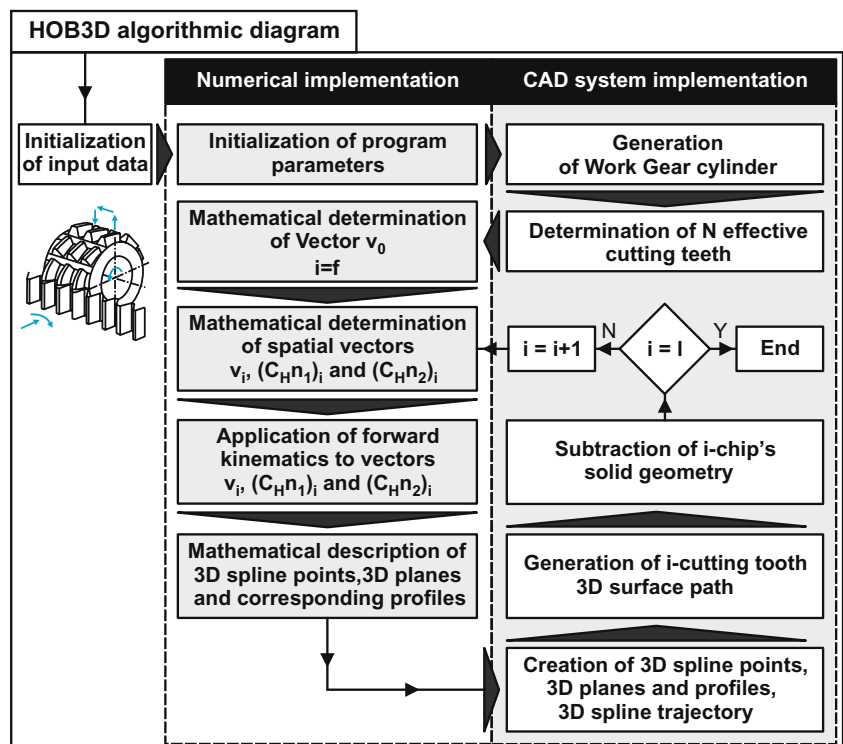
Fig. 4 Three-dimensional kinematics scheme in the CAD environment

fixed XYZ global system, determining the region where the cutting starts. Once the simulation parameters are settled, the work gear solid model is generated and the assembly of the effective cutting hob teeth is enabled. The moment that the gear hobbing simulation starts is considered as time zero. At this time ( $t=0$ ) the planes YZ and  $Y_h Z_h$  are parallel and their horizontal distance, steady for the whole simulation period, is set to:  $L_2 = (dh/2) + (dg/2) - t$ . The

distance  $L_2$  practically determines the cutting depth, user defined as an input parameter. To determine the setting angle  $\theta_s$ , the  $X_h Y_h Z_h$  hob coordinate system is rotated about the  $X_h$  axis, so that the simulation process becomes completely prescribed.

Using the spatial vector  $v_0$ , it is easy to compute the identification vectors  $v_i$  of each of the N effective teeth relatively to  $v_0$ , taking into account the hob geometrical

Fig. 5 Algorithmic diagram of the program HOB3D



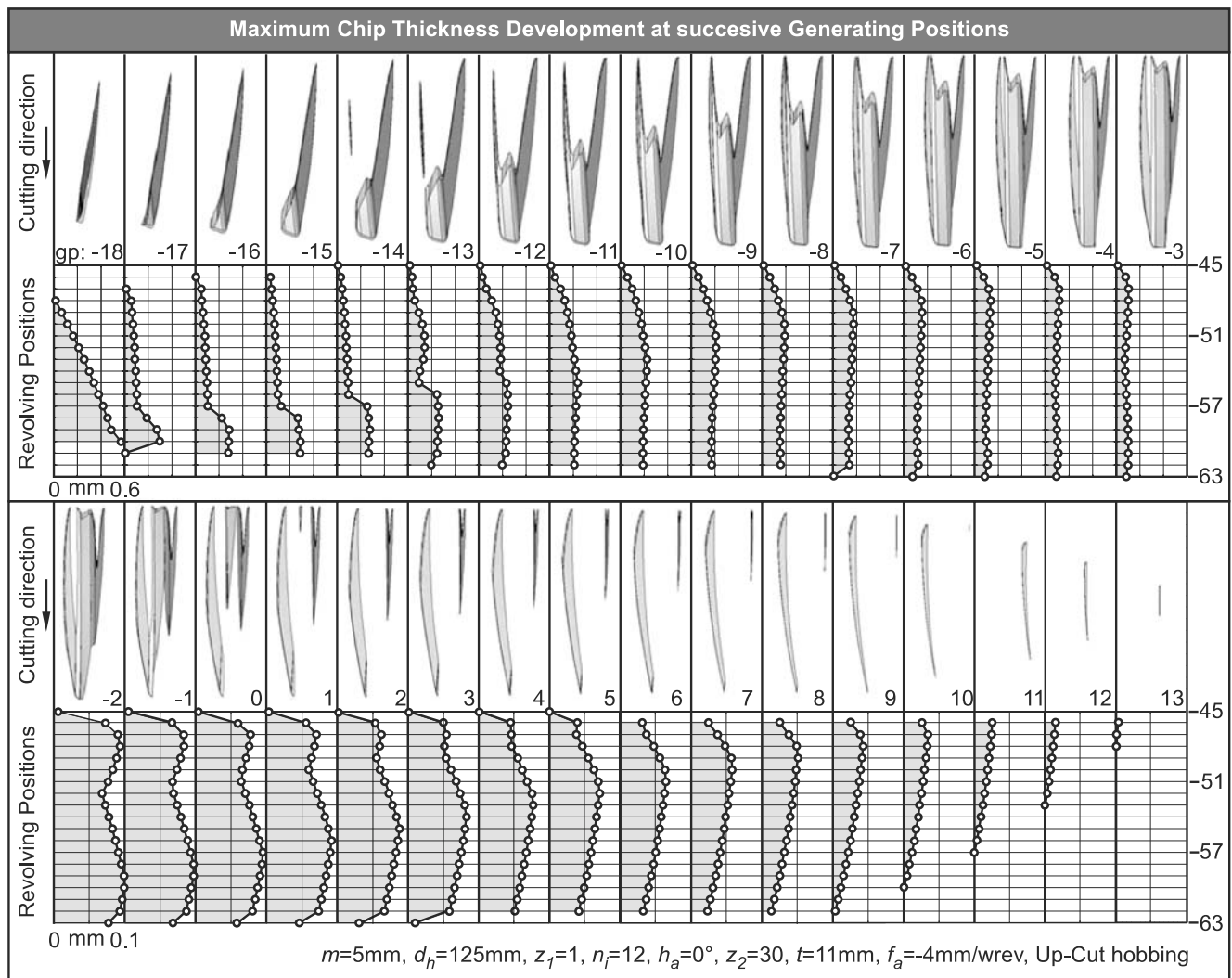


Fig. 6 Maximum chip thickness on the revolving positions of every generating position of a full work cycle

input parameters. The independent parameter  $\theta_1$  counts the rotational angle of hob tool about its axis  $Y_h$  during the cutting simulation. The parameter  $\theta_2$  declares the rotational angle of the hob tool about the work gear and  $f_a$  the axial feed of the hob.  $\theta_2$  and  $f_a$  are dependent from  $\theta_1$  and their values are determined according to the values of  $\theta_1$  angle (see also the upper part of Fig. 3). The forward kinematics of each of the  $N$  effective cutting hob teeth occur in one gear tooth space (gap). Hereby, after the determination of  $v_0$  and considering that the identification vector of the first of the  $N$  cutting hob tooth  $v_f$  is determined relatively to  $v_0$ , the forward kinematics are firstly applied to  $v_f$  and sequentially to the following vectors  $v_i$ , until the last cutting hob tooth of the work cycle  $v_l$ , simulating precisely the real manufacturing process.

In case of simulating helical gears fabrication, a differential angular amount is added on the rotating system of the gear, in order to increase or decrease the angular velocity of the rotating workpiece, ensuring the proper meshing of the hob-cutting and gear-cut angles. Depending

on the type of the hobbing process a new angular parameter  $d\theta$  has to be inserted to the whole kinematical chain for the acceleration or deceleration of  $\theta_2$ . The calculation of the parametrical value of  $d\theta$  is taking place on the pitch circle as it is detailed schematically presented in the lower part of Fig. 3, constituting a section of significant importance.

As illustrated at Fig. 4, the prescribed kinematics chain is used for the construction of a three-dimensional spline path in the CAD environment. This spline path occurs from the interpolation of points generated from the  $v_i$  vector of the cutting hob teeth, that is properly transformed and rotated by the help of the simulation parameters  $\theta_1$ ,  $\theta_2$  and  $f_a$ . Following the same tactic, the unit vectors  $(C_{Hn1})_i$  and  $(C_{Hn2})_i$ , described in the same Figure, are shifted and rotated for the generation of a plane properly positioned into the three-dimensional space, for every revolving position of the  $i$ -th cutting tooth.

The profile of the cutting hob tooth is formed on the two-dimensional space that is created by each one of these

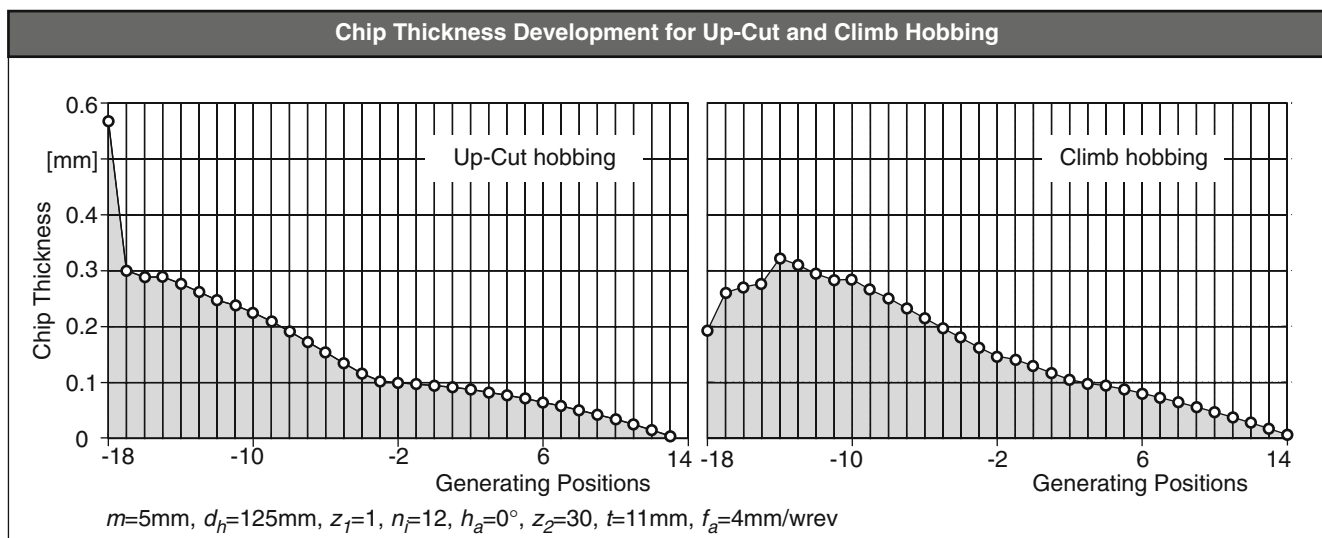


Fig. 7 Maximum chip thickness of the generating positions of a full work cycle for UC and CL gear hobbing cases

spatial planes, as presented in the middle of Fig. 4. By the proper lofting of the constructed open profiles following the rail of the constructed spatial spline, a three-dimensional open surface is created in one gear-gap tooth space. This surface path represents the generating position of the  $i$ -th cutting tooth and bounds its penetrating volume into the workpiece. With the aid of this surface path, the solid geometry of a chip is identified for every generating position, using the Boolean operations and the graphics capabilities of the CAD environment. The chip geometry is restricted by the external volume of the instantly formed working gear gap, bounded outside the created surface. The identified solid geometry is then subtracted from the workpiece leading to the generation of the continuous three-dimensional solid geometries of the chip and the remaining work gear. Because of the output form of the solid resulting parts of the simulation process, any kind of post-processing is primitively enabled. As can be seen at the lower right section of Fig. 4 in detail A, the maximum thickness of an extracted solid geometry of a chip at a certain revolving position is detected. All of the images presented in Fig. 4 were captured from the CAD environment during a simulation performed from HOB3D. The words, phases and arrows were added afterwards with the help of commercial image processing software for the better explanation of the images.

All of the previously mentioned simulation tasks are controlled by the developed program HOB3D that manipulates the modeling capabilities of the CAD system, forcing the generation of the geometrical entities in it, collecting the occurring geometrical data from it, and making all of the programmed numerical calculations. The continuous interaction of the CAD system with the numerical calculations environment of the program is algorithmically described at

Fig. 5. After the insertion of the input data from the user the program parameters are initialized. The work gear cylinder geometry is generated and the number  $N$  of the effective cutting teeth is computed. The spatial vector  $v_0$  is mathematically determined. The cutting tooth number parameter  $i$  is set to  $f$  (first cutting tooth number) and the vector  $v_i$  and the correspondent unit vectors  $(C_H n_1)_i$  and  $(C_H n_2)_i$ , essential for the construction of the spatial planes, are relative to  $v_0$  mathematically determined. The forward kinematics of the hobbing procedure is applied to these vectors. The resulting numerical data, prescribing the 3D spline points and the 3D planes, are used for the generation of the corresponding entities in the CAD environment. The generated 3D points are interpolated for the construction of the 3D spline in the CAD environment. For each created spatial plane, the correspondent tooth profile is mathematically formed and sketched in the CAD system. The profiles are lofted properly, following the 3D spline trajectory forming the 3D surface path of the  $i$ -cutting tooth. The solid geometry included in the spatial surface is subtracted from the work gear and saved as the  $i$ -chip geometry (see the enlargement detail of Fig. 4). The  $i$ -counter takes the value  $i+1$  and the same procedure is repeated until  $i$  became equal to  $l$  (last cutting tooth number).

For the reduction of the computational effort and time, the overall rotation of the hob about its axis  $Y_h$  is restricted from 0 to 180 degrees ( $0^\circ \leq \theta_l \leq 180^\circ$ ) for every generating position of each effective cutting hob tooth  $i$ . This way only the motions that affect the resulting solid geometries are taking place, without any influence to the process sufficiency, during the entire simulation process. After the completion of the sequential construction of every spatial surface and the subtraction of the chip solid geometries, the gear gap is generated, formed by the collective work of every generating position.

### 4 HOB3D simulation results

The developed program HOB3D is used for the simulation of manufacturing of spur and helical gears, and its post-processing code is used for the determination of the solid chip thickness development. The proposed program was verified and validated in a previous research work [18], by the usage of the resulting three-dimensional solid geometries of the gear gaps generated by HOB3D. These gap profiles were compared to the standard ones introduced by Petri [19] and DIN 3972 [20] and the calculated mean error was less than 10 μm for the working depth of produced gears. Such negligible deviations satisfy the computational accuracy expectations, and verify the sufficiency of the developed code.

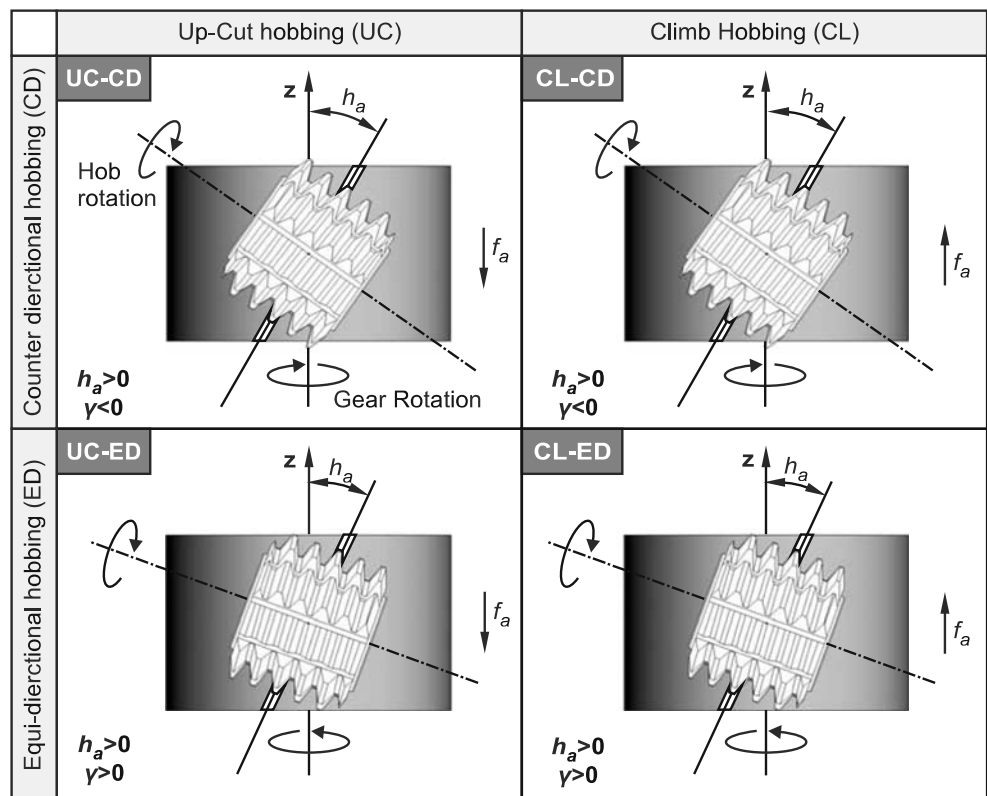
#### 4.1 Simulation of the manufacturing process of spur gears

HOB3D is used for the simulation of manufacturing of a spur gear. The input data of the UC case processed and the output chip solid geometries of every generating position are presented in Fig. 6. The cutting direction of the hob tool is indicated at the left of the figure and the observation of chips is taking place from the site of the hob. Examining the three-dimensional solid geometries of the displayed chips, we see that it is obvious that so much as the extreme geometrical changes of the chip shapes are sufficiently determined, even if it is parted from more than one domain.

The developed post-processing code of the program is used for the maximum thickness measurement of every chip of the work cycle on each revolving position. Ninety-one (0 to 90) assigned revolving positions (rp) that belong to the kinematics of each generating position (gp) are used. In case of intersection of a spatial plane of an rp with the solid geometry of the chip, the maximum thickness ( $h_{max}$ ) is identified and recorded. This sequence leads to the generation of the maximum thickness diagrams that are presented below each chip at Fig. 6. As shown in the right of the diagrams the measurement is taking place at a number of nineteen revolving positions that range from the 45th to the 63th rp.

For the improvement of the visualization of the resulting diagrams, Fig. 6 is parted from two sections (upper and lower). At the upper section of the figure the sixteen first generated chips are presented, corresponding to the generating positions -18 to -3. The range of the maximum thickness at these diagrams is from 0 to 0.6 mm. As can be observed, the values of the chip thicknesses are close to zero at the first revolving positions and approach their maxima close to the end of the chip. If the chip generated at the position -18 is excluded because of the supreme thickness value of 0.57 mm that reveals from the chip of the generating position -17 until -3 the maximum thicknesses are oscillating from 0.3 mm to 0.1 mm with a descending rate. The reduction of the values of the chip thicknesses holds on and for the chips generated at the

**Fig. 8** Schematic representation of four different gear hobbing strategies



positions  $-2$  to  $13$ . That is the reason why the range of the diagrams at these next sixteen generating positions (gp:  $-2$  to  $13$ ) presented in the lower part of the figure, varies from  $0$  to  $0.1$  mm. It can be easily observed that the supreme values of the chip thicknesses are following the same descending route as the first sixteen and from the higher value of  $0.1$  mm that appears at the generating position  $-2$ , the work cycle stops at the generating position  $13$ , where the maximum chip thickness value is very close to zero.

The simulation data of the UC case are reused for the approximation of the results of a CL case by changing only the sign of the axial feed ( $f_a$ ) input. After the evaluation of the chip solid geometries, the post-processor of HOB3D is mobilized for the measurement of the maximum chip thickness, in the same sense that was previously described. The maximum thicknesses of each generating position are recorded and plotted to Fig. 7 for both of the UC and CL cases.

As shown in the two graphs of Fig. 7, the first effective (penetrating) generating position of both of the cases is the one prescribed from the cutting hob tooth with  $i=-18$  ( $v_j=v_{-18}$ ). For the UC case the last effective generating position

is the one prescribed from the cutting hob tooth with  $i=13$  ( $v_j=v_{13}$ ) while for the CL case  $v_j=v_{14}$ . Except from the first generating position of the UC where the measured maximum chip thickness approximates the value of  $0.6$  millimetres, it is observed that the measured results for both of the cases are oscillating in a range of  $0$  mm to  $0.3$  mm approximately. The supreme values of the measured maximum thicknesses of the UC and CL cases is  $0.57$  mm at gp= $-18$  and  $0.32$  mm at gp= $-14$ , respectively.

#### 4.2 Simulation of the manufacturing of helical gears

In the case of manufacturing helical gears, four different hobbing strategies may be prescribed, depending on the process parameters that will be chosen, as it was thoroughly described at the HOB3D modeling procedure paragraph. The schematic representation of these strategies for the manufacturing process of a helical gear with positive helix angle ( $h_a > 0^\circ$ ) is presented in Fig. 8.

HOB3D is used for the simulation of manufacturing of a helical gear with helix angle  $h_a=30^\circ$  by these four strategies. The values of the input data of the examined

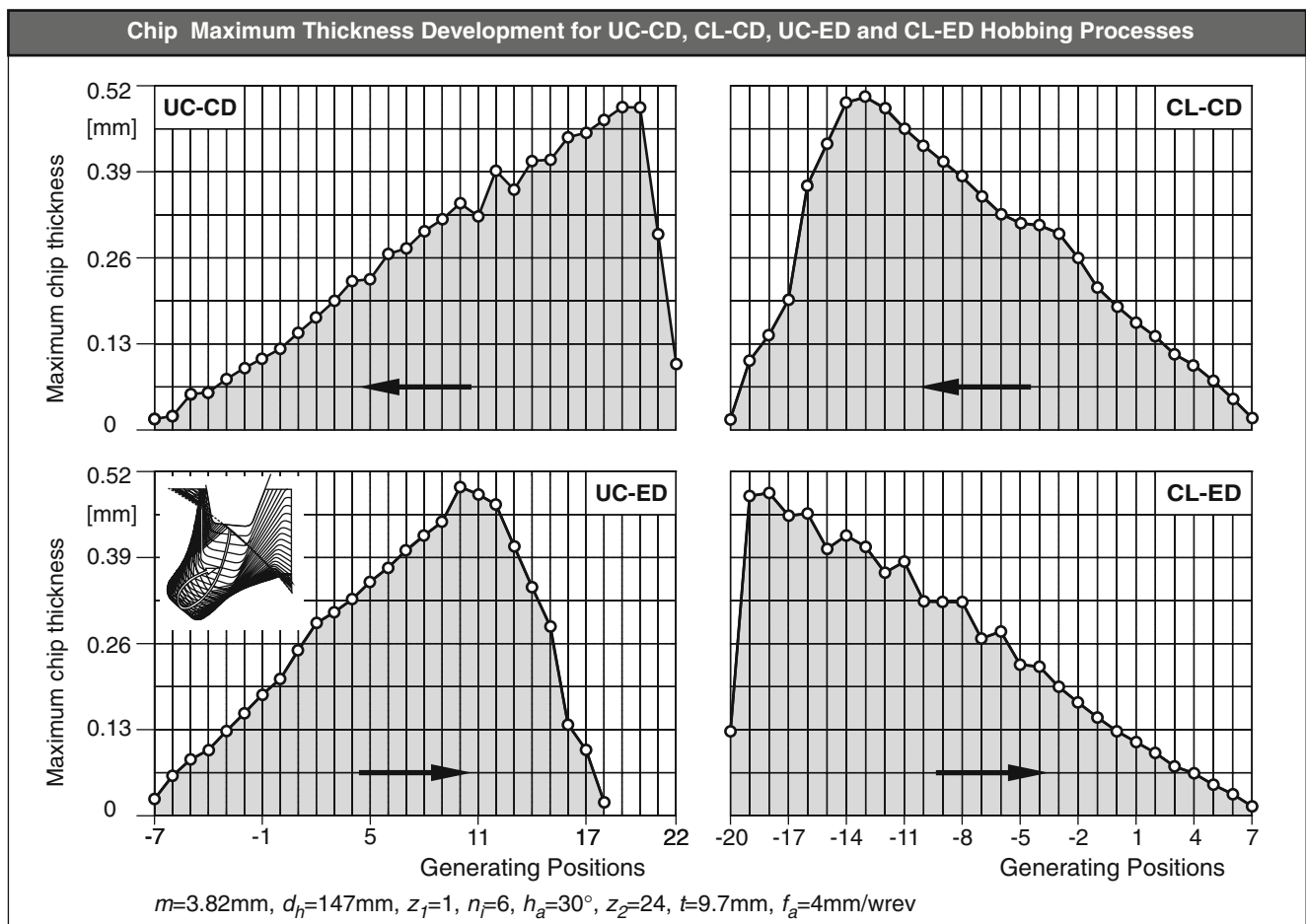


**Fig. 9** Maximum chip thickness graphical representation of the generating positions of a full work cycle for UC-CD, CL-CD, UC-ED and CL-ED gear hobbing cases



cases are identical for each one of them except from the tool helix angle ( $\gamma$ ) and the axial feed ( $f_a$ ). The sign of these parameters denotes the hobbing strategy of each case, as presented in Figs. 8 and 9.

After the evaluation of the chip solid geometries for each one of the four different strategies, the post-processor of HOB3D is mobilized for the measurement of the maximum chip thickness, by the same tactic that was formerly described. The maximum thicknesses of each generating position are recorded and plotted to Fig. 9 for the UC-CD, CL-CD, UC-ED and CL-ED test cases.

As shown in the four graphs of Fig. 9, the first effective (penetrating) generating position of the UC-CD case is the one prescribed from the cutting hob tooth with  $i=22$  ( $v_j=v_{22}$ ) and the last from  $i=-7$  ( $v_l=v_{-7}$ ). This is the reason why the black arrow in the graph is pointing to the left so as to denote the sequence of the cutting teeth. The same holds for the CL-CD case were  $v_j=v_7$  and  $v_l=v_{-20}$ . This is a result of the left-hand rotation of the workpiece and the numbering of the hob tool teeth that is used. As can be seen in the two graphs of the -ED cases, the arrow is pointing to the reverse direction (from left to right) because of the right-hand

rotation of the gear and the numbering of the hob tool teeth that is used. At the UC-ED case  $v_j=v_{-7}$  and  $v_l=v_{18}$  and at the CL-ED case  $v_j=v_{-20}$  and  $v_l=v_7$ .

It should be observed that for all of the four cases the maximum chip thicknesses are oscillating in the same range of 0 mm to 0.52 mm, and the supreme value of each one of them approximates the value of the 0.5 mm. Also, it should be noted that the diagrams of the UC-CD case and CL-ED case appear the same behavior of oscillations and the same holds for the CL-CD and UC-ED cases.

The 3D chip solid geometries, produced from HOB3D, for the simulation of the UC-ED gear hobbing process, are presented in Fig. 10. The input data of the case processed are presented in the bottom of the Figure. The cutting direction of the hob tool is indicated at the left of the Figure and the observation of chips is taking place from the site of the hob. Examining the three-dimensional solid geometries of the displayed chips, we find it obvious that so much as the extreme geometrical changes of the chip shapes are sufficiently determined, even when the chip is parted from more than one domain.

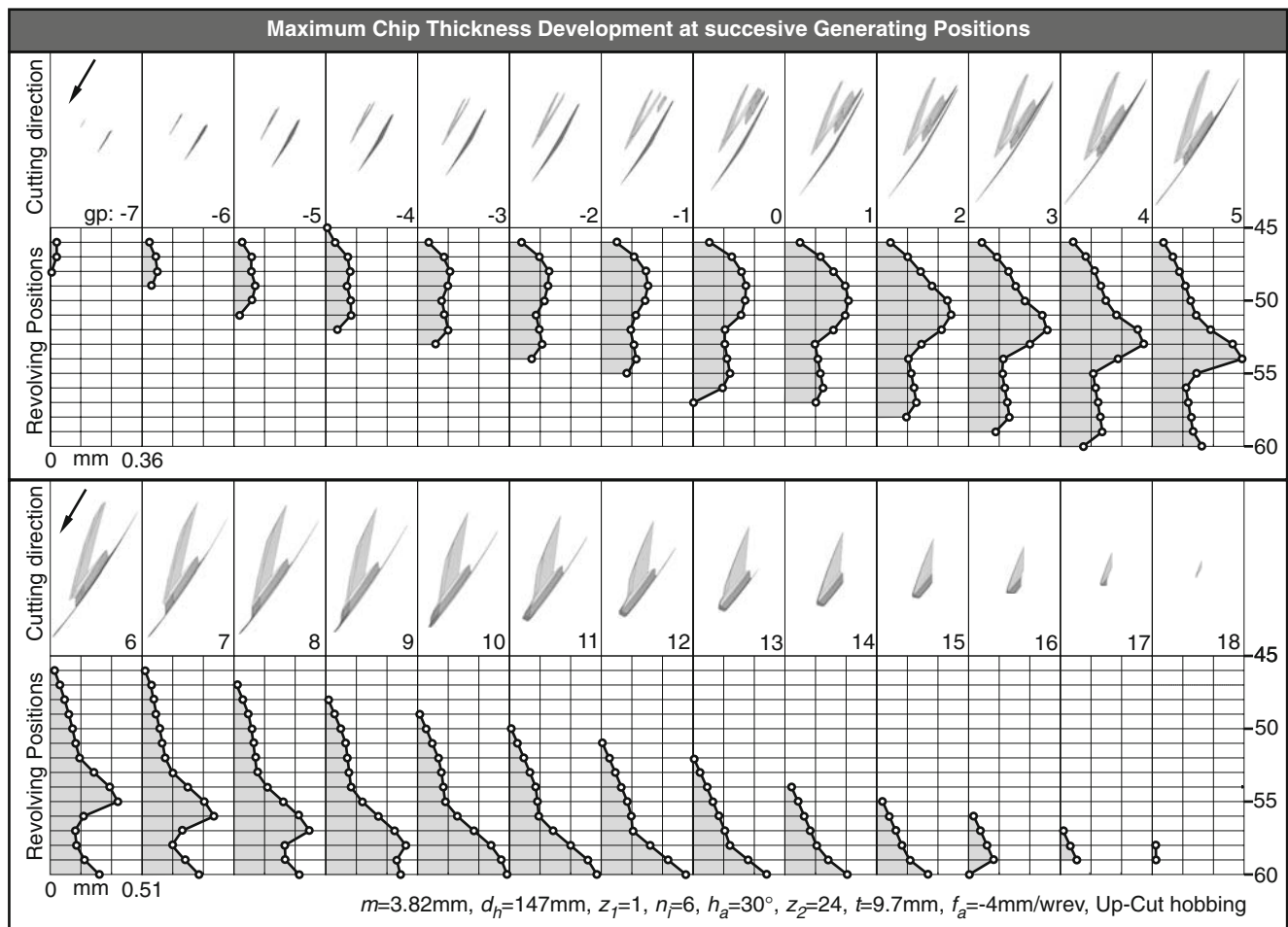


Fig. 10 Maximum chip thickness on the revolving positions of every generating position of a full work cycle of a UC-ED gear hobbing process

The developed post-processing code of the program is used again for the maximum thickness measurement of every chip of the work cycle on each revolving position. Ninety-one (0 to 90) assigned revolving positions that belong to the kinematics of each generating position are used. In case of intersection of a spatial plane of a revolving position with the solid geometry of the chip, the maximum thickness is identified and recorded. This sequence leads to the generation of the maximum thickness diagrams that are presented below each chip at Fig. 10. As shown in the right of the diagrams, the measurement is taking place at a number of sixteen revolving positions that range from the 45th to the 60th revolving position.

For the improvement of the visualization of the resulting diagrams, Fig. 10 is parted from two sections (upper and lower). At the upper section of the figure the first 13 generated chips are presented, corresponding to the generating positions  $-7$  to  $5$ . The range of the maximum thickness at the diagrams is from  $0$  to  $0.36$  mm. As can be observed, the values of the chip thicknesses from the generating position  $-7$  to  $5$  have an ascending rate and from a maxima value of  $0.025$  mm at the gp: $-7$  approach the value of  $0.36$  mm at the gp:  $5$ . As can be observed, these maximum thickness values appear to a position close to the middle of the successive revolving positions. The increment of the values of the chip thicknesses holds on and for the chips generated at the positions  $6$  to  $10$ . That is the reason why the range of the diagrams at the next thirteen (gp:  $6$  to  $18$ ) generating positions, presented in the lower part of the figure varies from  $0$  to  $0.51$  mm. It can be observed that the maximum value of the chip thickness approaches the supreme value of  $0.51$  mm at the last revolving position of the chip generated at the position  $10$ . From the generating position  $11$ , the maximum thickness values have a descending order, until the last (gp:  $18$ ) where the maximum chip thickness value is very close to zero.

## 5 Conclusion

In the current research work, an advanced and validated simulation program called HOB3D, based on a commercial CAD environment, was proposed and used for the simulation of the gear hobbing process, for the manufacturing of spur and helical gears. In contradistinction to former research attempts, in the present investigations, the kinematics of gear hobbing is directly applied in one-tooth three-dimensional space by the construction of spatial surface paths, for every generating position. The kinematics involves the rotations and displacements of the two rolling parts (hob and work gear) for every manufacturing case of gear hobbing process. These three-dimensional surface paths are used to split the subjected volume and directly

create the chip and the remaining work gear continuous solid geometries.

Considering the quality and the output format of the resulting solid geometries enables the direct post-processing of them for further investigations eliminating the need of inter or extrapolations required until now. The thicknesses of the extracted chip solid geometries are measured, recorded and plotted by HOB3D to graphs for two different types of spur gear manufacturing and four different types of the manufacturing of a helical gear. The results of the present work hold significant industrial and research interest, including the accurate prediction of dynamic behavior and tool wear development in gear hobbing procedure. By the completion of the research work (prediction of cutting forces, wear, tool failure, etc), and the fulfilment of the research software HOB3D, it may constitute a part module of a CAD system.

## References

1. Klocke F, Klein A (2006) Tool life and productivity improvement through cutting parameter setting and tool design in dry high-speed bevel gear tooth cutting. *Gear Technol*:40–48
2. Rech J (2006) Influence of cutting edge preparation on the wear resistance in high speed dry gear hobbing. *Wear* 216/5–6:505–512 DOI 10.1016/j.wear.2005.12.007
3. Rech J, Djouadi MA, Picot J (2001) Wear resistance of coatings in high speed gear hobbing. *Wear* 250/Part1:45–53
4. Kim DH (2001) Geometry of hob and simulation of generation of the cylindrical gears by conventional or climb hobbing operation. *Proceedings of the I MECH E Part D Journal of Automobile Engineering* 215/4:533–544
5. Fan Q (2006) Computerized modeling and simulation of spiral bevel and hypoid gears manufactured by gleason face hobbing process. *J Mech Des* 128/6:1315–1327 DOI 10.1115/1.2337316
6. Sulzer G (1974) Leistungssteigerung bei der Zylinderradherstellung durch genaue Erfassung der Zerspankinematik, Dissertation, TH Aachen
7. Gutman P (1988) Zerspankraftberechnung beim Waelzfraesen, Dissertation, TH Aachen
8. Venohr G (1985) Beitrag zum Einsatz von hartmetall Werkzeugen beim Waelzfraesen, Dissertation, TH Aachen
9. Joppa K (1977) Leistungssteigerung beim Waelzfraesen mit Schnellarbeitsstahl durch Analyse, Beurteilung und Beeinflussung des Zerspanprozesses, Dissertation, TH Aachen
10. Tondorf J (1978) Erhoehung der Fertigungsgenauigkeit beim Waelzfraesen durch systematische Vermeidung von Aufbauschneiden, Dissertation, TH Aachen
11. Antoniadis A (1988) Determination of the impact tool stresses during gear hobbing and determination of cutting forces during hobbing of hardened gears, Dissertation, Aristoteles University of Thessaloniki
12. Antoniadis A, Vidakis N, Bilalis N (2002) Fatigue fracture investigation of cemented carbide tools used in gear hobbing, Part I: fem modeling of fly hobbing and computational interpretation of experimental results. *ASME J Manuf Sci Eng* 124/4:784–791 DOI 10.1115/1.1511172
13. Antoniadis A, Vidakis N, Bilalis N (2002) Fatigue fracture investigation of cemented carbide tools used in gear hobbing, Part

- II: the effect of cutting parameters on the level of tool stresses - a quantitative parametric analysis. *ASME J Manuf Sci Eng* 124/4:792–798 DOI [10.1115/1.1511173](https://doi.org/10.1115/1.1511173)
14. Sinkevicius V (1999) Simulation of gear hobbing geometrical size. *Mechanika (Kaunas University of Technology Journal)* 5 (50):34–39
  15. Sinkevicius V (2001) Simulation of Gear Hobbing forces. *Mechanika (Kaunas University of Technology Journal)* 2 (28):58–63
  16. Komori M, Sumi M, Kubo A (2004) Method of preventing cutting edge failure of hob due to chip crush. *JSME Int J Ser C Mech Syst Mach Elem Manuf* 47(4):1140–1148
  17. Komori M, Sumi M, Kubo A (2004) Simulation of hobbing for analysis of cutting edge failure due to chip crush. *Gear Technol*, 64–69
  18. Dimitriou V, Vidakis N, Antoniadis A (2007) Advanced computer aided design simulation of gear hobbing by means of 3-dimensional kinematics modeling. *ASME J Manuf Sci Eng* 129 \5:911–918 DOI [10.1115/1.2738947](https://doi.org/10.1115/1.2738947)
  19. Petri H (1975) Zahnhuß - Analyse bei außenverzahnten Evolventenstirnraedern: Teil III Berechnung. *Antriebstechnik* 14(5):289–297
  20. DIN 3972 (1992) Bezugsprofile von Verzahnwerkzeugen fuer Evolventen-Verzahnungen nach DIN 867. Taschenbuch 106, Beuth Verlag, Berlin